PESSTO SSDR3 : ESO Phase 3 Data Release Description

Data Collection	PESSTO
Release Number	4
Data Provider	Stephen J. Smartt (PI of PESSTO)
Date	09.12.2016

Abstract

PESSTO (Public ESO Spectroscopic Survey of Transient Objects) began in April 2012 on the New Technology Telescope using the instruments EFOSC2 and SOFI. We typically target supernovae and optical transients brighter than 20.5^{m} for classification and select science targets detailed follow-up. We use standard EFOSC2 setups providing spectra with resolutions of 13-17Å between 3680-10320Å. A subset of the brighter science targets are selected for SOFI spectroscopy with the blue and red grisms (resolutions 23-33Å) and imaging with broadband JHK_s filters. In the following, we define SSDR3 as the set of data products from April 2012 to April 2016, covering the first four years of PESSTO operations. This Release number 4 includes the EFOSC2 and SOFI spectra and the reduced SOFI images obtained during the first four years of PESSTO operations. Updated versions of the PESSTO Transient and Multi-Lightcurve catalogues will be released soon.

Overview of Observations

PESSTO has been allocated 90 nights per year, in visitor mode, on the ESO NTT. There are no observations planned during the months of May, June and July due to the Galactic centre being at optimal right ascension. These three months make it more difficult to search for extragalactic SNe and there is large time pressure from the ESO community for Milky Way stellar science. PESSTO typically has been allocated 10 nights per month split into three sub-runs of 4N, 3N and 3N. Typically the middle sub-run is dark time, while the two others are grey/bright with the moon up for around 50% of the time. The instruments used are EFOSC2 and SOFI and both spectroscopy and imaging modes are employed. The PESSTO collaboration host public webpages with useful information in the form of night reports, observing conditions, observing with the NTT, and the data reduction pipeline. This information is updated during the survey and users should read this document with the information on www.pessto.org and the wiki pages that the homepage points to. A summary of the spectroscopic data setups is given in Tables 1 and 2. The science target selection strategy is described in detail in Smartt et al. (2015)

Table 1. PESSTO settings for EFOSC2 spectroscopy. The blocking filter OG530 is used only (and always) for Gr#16. The 1" slit projects to 3.5 binned pixels. The column headed Arclines indicates the number of lines used. The RMS is the typical residual for the wavelength calibration solution.

Grism	Wavelength (Å)	Filter (blocking)	Dispersion (Åpix^{-1})	Resolution (Å for 1" slit)	Arclines (number)	RMS (Å)
#13	3650 - 9250	none	5.5	18.2	13-15	0.10-0.15
#11	3345 - 7470	none	4.1	13.8	9	0.10-0.15
#16	6000 - 9995	OG530	4.2	13.4	11-14	0.05-0.10

Table 2. PESSTO settings for SOFI spectroscopy. The 1" slit projects to 3.4 pixels FWHM, measured from arc lines. The column headed Arclines indicates the number of lines used. The RMS is the typical residual for the wavelength calibration solution. The order blocking filters used are 0.925μm (GBF) and 1.424μm (GRF) "cut-on" filters.

Grism	Wavelength (μm)	Filter (blocking)	Dispersion (Å pix^{-1})	Resolution (Å for 1" slit)	Arclines (number)	RMS (Å)
Blue	0.935 - 1.654	GBF	6.95	23	12-14	0.1-0.2
Red	1.497 - 2.536	GRF	10.2	33	7-8	0.2-0.5

Release Content

PESSTO observes single targets in long-slit mode and selects targets for two purposes as described in Smartt et al. (2015). The first is to classify targets as early as possible after discovery. The main feeder survey for PESSTO has been the La Silla QUEST survey (LSQ), as described in Baltay et al. (2013) and which ceased operations in April 2016, but PESSTO takes targets from many different public surveys. These "classification" spectra are taken with Grism#13 and typically we aim for signal-to-noise in the continuum between 10-20 depending on the magnitude of the source. The main purpose is to reliably screen targets to determine their classification and redshift. The science goal of PESSTO (Smartt et al. 2015) is detailed follow-up and time series spectroscopic monitoring of supernovae at the extremes of the known population e.g. the most luminous, the faintest, the fast declining etc. Hence the screening classification spectra are necessarily kept short in order to minimize the time observing normal supernovae and maximize the time available for scientific follow-up.

In the first fours years, PESSTO has taken spectra of 1168 distinct objects. From this list, 161 supernovae (10 of which are super-luminous supernovae), 2 supernova imposters, 3 Tidal Disruption Events, 1 unclassified objects and 1 AGN were picked as interesting science targets and these were scheduled for follow-up time series EFOSC2 optical spectroscopy, with the brightest also having SOFI spectra. A summary of these 168 PESSTO Key Science targets and the spectral data sets taken is given in Table 3. The total number of spectra released for these 168 "PESSTO Key Science" targets are 1753 EFOSC2 spectra and 224 SOFI spectra (a total of 1977). These EFOSC2 numbers include the first classification spectra taken.

PESSTO has used EFOSC2 in imaging mode to take acquisition images of many of the targets before a spectrum is taken and in some cases multi-colour photometry is taken. Smartt et al. (2015) describes the rationale for lightcurve construction for PESSTO science targets, which are typically bright enough to be done with smaller aperture facilities. SOFI imaging is nearly always taken when SOFI near infra-red spectra are taken.

In total the SSDR3 contains 21.29GB of data and the numbers of images and spectra are given in Table 4. In total there are 2851 EFOSC2 spectra released.

These include the 1753 EFOSC2 spectra of Table 3. The remaining 1098 EFOSC spectra relate to 1000 objects for which we took spectra but did not pursue a detailed follow-up campaign. There are more spectra than objects simply due to the fact that in some cases PESSTO took more than one spectrum for classification due to either low signal-to-noise in the first spectrum, or ambiguous classifications that needed further spectra to allow a secure analysis. Generally, the first spectrum taken of an object was enough for a classification. However there were circumstances in which further spectra were needed due to either low signal-to-noise, or a real ambiguity. The most common cause of ambiguity in classification are objects showing featureless blue continua. These are usually young type II SNe, but can be Galactic CVs, tidal disruption candidates, or moderate redshift superluminous supernovae. In these cases further spectra usually show spectral features to allow redshift and classifications. The classifications released by PESSTO are based on the set of early spectra taken.

PESSTO has taken EFOSC2 images which include multi-colour follow-up images of science targets, EFOSC2 acquisition images, and standard star fields (fields are defined in Smartt et al. 2015). These EFOSC2 images will be astrometrically and photometrically calibrated (as far as the small field of view of EFOSC2 will allow). The raw images are available in the ESO archive and on www.pessto.org. We plan to associate these reduced and calibrated images with the archive spectra products in the future.

In some cases the astrometric position of the science target on SOFI (or the EFOSC2) images can be of order 0.5 – 1.5 arcsec different to that recorded in the headers of the 1D spectral files. The coordinates in the 1D spectral files are those of the target and these are taken from a range of surveys which can have minor, but measureable, errors in the absolute astrometry. The coordinates in the SOFI and (future) EFOSC2 images are likely to be as good if not better than those originally provided from the feeder surveys, but discrepancies are typically less than 1.5 arcseconds.

Table 3: PESSTO SSDR3 Key Science targets. These targets were selected for detailed follow-up in the first four years of survey operations, initially with EFOSC2 and with SOFI when possible. The numbers refer to the numbers of epochs of spectra taken with each Grism. Gr11, GR13 and Gr16 refer to the EFOSC2 grisms and GB, GR refer to the SOFI grisms.

Target	Type	Number of Spectra	Comments
SN2009ip	SN IIn	27xGr11, 5xGr13, 21xGr16, 8xGrGB, 6xGrGR	Fraser et al. (2013), Fraser et al. (2015)
SN2012fr	SN Ia	15xGr11, 2xGr13, 15xGr16, 10xGrGB, 9xGrGR	Childress et al. (2013), Childress et al (2015)
SN2012ec	SN IIP	14xGr11, 2xGr13, 11xGr16, 11xGrGB, 4xGrGR	Maund et al. (2013), Barbarino et al. (2015), Jerkstrand et al. (2015)
SN2015F	SN Ia	12xGr11, 1xGr13, 11xGr16, 9xGrGB, 9xGrGR	
ASASSN-14ha	SN II	14xGr11, 4xGr13,	

		13xGr16, 4xGrGB, 4xGrGR	
SN2013ej	SN II	13xGr11, 2xGr13, 13xGr16, 5xGrGB, 5xGrGR	Yuan et al. (2016)
SN2014cx	SN II	7xGr11, 13xGr13, 7xGr16, 5xGrGB, 4xGrGR	
SN2013K	SN IIP	6xGr11, 18xGr13, 7xGr16, 1xGrGB	
LSQ13fn	SN IIn	13xGr11, 9xGr13, 6xGr16	Polshaw et al. (2016)
SN2012dy	SN IIb	12xGr11, 6xGr13, 9xGr16	
LSQ14an	SLSN Ic	9xGr11, 9xGr13, 9xGr16	
SN2015L	SN I	13xGr11, 1xGr13, 13xGr16	
SN2012ca	SN IIn	18xGr13, 5xGrGB, 3xGrGR	Inserra et al. (2013, 2016)
SN2013gr	SN Ia	11xGr11, 5xGr13, 10xGr16	
SN2013fc	SN IIn	9xGr11, 7xGr13, 6xGr16, 2xGrGB, 2xGrGR	Kangas et al. (2016)
SN2014eg	SN Ia	12xGr11, 1xGr13, 10xGr16, 2xGrGB, 1xGrGR	
SN2012hs	SN IIb	7xGr11, 7xGr13, 7xGr16, 3xGrGB, 1xGrGR	
LSQ15adm	SN I-CSM	11xGr11, 1xGr13, 8xGr16, 2xGrGB, 2xGrGR	
PS15br	SN Ic-p	4xGr11, 16xGr13, 4xGr16	Inserra et al. (2016)
LSQ14mo	SLSN Ic	5xGr11, 14xGr13, 3xGr16	
SN2013ao	SN Ia	11xGr11, 1xGr13, 9xGr16	Maguire et al. (2013)
SN2016adj	SN II	5xGr11, 6xGr16, 5xGrGB, 5xGrGR	
SN2013ak	SN IIb	8xGr11, 6xGr16, 3xGrGB, 3xGrGR	
LSQ12dwl	SN Ic-p	2xGr11, 7xGr13, 2xGr16, 5xGrGB, 4xGrGR	
LSQ15kp	SN II-p	5xGr11, 10xGr13, 5xGr16	
SN2015D	SN IIP	11xGr11, 1xGr13, 8xGr16	
OGLE15xl	SLSN Ic	2xGr11, 16xGr13, 2xGr16	
SN2015H	SN Ia	5xGr11, 6xGr13, 5xGr16, 3xGrGB, 1xGrGR	Magee t al. (2016)
PS15ae	SN Ic-p	5xGr11, 4xGr13, 5xGr16, 4xGrGB, 1xGrGR	Nicholl et al. (2016a, 2016b), Jerkstrand et al. (2016)
PS15cww	SN IIn	8xGr11, 8xGr13, 2xGr16, 1xGrGB	
OGLE-2013-SN-016	SN IIn	9xGr11, 1xGr13, 7xGr16	
LSQ14pt	SN IIn	5xGr11, 1xGr13, 11xGr16	
ASASSN-14lp	SN Ia	8xGr11, 1xGr13, 8xGr16	
ASASSN-14il	SN IIn	4xGr11, 1xGr13, 4xGr16, 5xGrGB, 3xGrGR	
LSQ12hxg	SN II	5xGr11, 8xGr13, 3xGr16	
LSQ12gdj	SN Ia-p	7xGr11, 7xGr16, 1xGrGB, 1xGrGR	Scalzo et al. (2013)
CSS121015-004244+132827	SLSN II	16xGr13	Benetti et al. (2013)
SN2013fs	SN IIP	8xGr11, 6xGr16, 1xGrGB, 1xGrGR	
LSQ14efd	SN I	2xGr11, 14xGr13	
ASASSN-15oi	TDE	5xGr11, 5xGr13, 5xGr16, 1xGrGB	

LSQ12dyw	TDE	1xGr11, 13xGr13, 1xGr16	
CSS140421-142042+031602	SN Ibn	3xGr11, 9xGr13, 3xGr16	Hosseinzadeh et al. (2016)
SN2013ew	SN Ia-p	6xGr11, 2xGr13, 7xGr16	
OGLE-2015-SN-035	SN II	1xGr11, 13xGr13, 1xGr16	
PS15cwo	SN II	7xGr11, 1xGr13, 7xGr16	
SN2013ai	SN II	3xGr11, 11xGr13	
SN2013bb	SN IIb	4xGr11, 6xGr13, 4xGr16	
PSNJ09204691-0803340	SN IIn	8xGr11, 6xGr16	
OGLE-2014-SN-073	SN II	14xGr13	
SSS130221-133330-194457	SN IIn	7xGr11, 6xGr13	
SN2013am	SN II	7xGr13, 3xGrGB, 3xGrGR	
SN2013ek	SN Ic	5xGr11, 1xGr13, 5xGr16, 2xGrGB	
NGC7552-OT	Imposter	6xGr11, 7xGr16	
OGLE-2012-SN-006	SN Ibn	1xGr11, 6xGr13, 1xGr16, 2xGrGB, 2xGrGR	Pastorello et al. (2015b)
SSS120810-231802-560926	SLSN Ic	12xGr13	Nicholl et al. (2014)
LSQ13ddu	SN I	4xGr11, 5xGr13, 3xGr16	
PSNJ15053007+0138024	SN Ia-p	7xGr13, 3xGrGB, 2xGrGR	
SN2016B	SN IIP	6xGr13, 3xGrGB, 3xGrGR	
SN2016X	SN IIP	4xGr11, 4xGr16, 2xGrGB, 2xGrGR	
LSQ12heq	SN IIn	4xGr11, 5xGr13, 2xGr16	
OGLE-2012-SN-040	SN Ia-p	3xGr11, 3xGr13, 3xGr16, 1xGrGB, 1xGrGR	
CSS130403-150213+103846	SN Ia	7xGr11, 1xGr13, 3xGr16	
LSQ14asn	SN Ic	8xGr11, 3xGr13	
CSS131110-023957-083124	SN II	5xGr11, 4xGr13, 2xGr16	(LSQ13cuw) Gall et al. (2015)
SN2013hx	SLSN II	4xGr11, 3xGr13, 4xGr16	Inserra et al. (2016)
SN2013dn	SN IIn	3xGr11, 5xGr13, 3xGr16	
SN2013fq	SN IIb	4xGr11, 1xGr13, 4xGr16, 1xGrGB, 1xGrGR	
LSQ14fxj	SLSN Ic	2xGr11, 7xGr13, 2xGr16	
SN2014dq	SN II	3xGr11, 4xGr13, 4xGrGB	
AT2015bm	SN II	11xGr13	
SN2012hr	SN Ia	3xGr11, 1xGr13, 3xGr16, 2xGrGB, 1xGrGR	Maguire et al. (2013)
LSQ12hot	SN IIn	1xGr11, 9xGr13	
OGLE-2013-SN-079	SN I	4xGr11, 4xGr13, 2xGr16	Inserra et al. (2015)
CSS130809-222004-213922	SN II	5xGr11, 3xGr13, 2xGr16	
ASASSN-15ga	SN Ia	3xGr11, 3xGr16, 2xGrGB, 2xGrGR	
SN2015ah	SN Ib-p	4xGr11, 4xGr16, 1xGrGB, 1xGrGR	
PS15cwz	SN Ia-p	4xGr11, 2xGr13, 4xGr16	
LSQ14gqk	SN Ic	1xGr11, 7xGr13, 1xGr16, 1xGrGB	
SN2015ap	SN Ib	5xGr11, 3xGr16, 1xGrGB, 1xGrGR	
ASASSN-15og	SN IIn-p	5xGr11, 5xGr16	
SN2012ht	SN Ia	3xGr11, 3xGr16, 2xGrGB, 1xGrGR	Maguire et al. (2013)

LSQ12gpw	SN Ia-p	4xGr11, 1xGr13, 4xGr16	
PSNJ15213475-0722183	SN IIn-p	6xGr11, 1xGr13, 2xGr16	
LSQ12dlf	SLSN Ic	1xGr11, 7xGr13, 1xGr16	Nicholl et al. (2014)
LSQ12fxd	SN Ia	4xGr11, 1xGr13, 4xGr16	
OGLE-2013-SN-100	SN II	8xGr13, 1xGr16	
NGC772-OT1	Imposter	1xGr13, 7xGr16, 1xGrGB	
ASASSN-14ko	SN IIn	4xGr11, 1xGr13, 4xGr16	
ASASSN-14lw	SN Ia	4xGr11, 4xGr16, 1xGrGB	
ASASSN-14hu	SN Ia	9xGr13	
ASASSN-15oz	SN II	5xGr13, 2xGrGB, 2xGrGR	
MASTERJ003918.04+035659.6	SN Ia	3xGr11, 1xGr13, 3xGr16, 1xGrGB, 1xGrGR	
SN2016aiy	SN IIn	4xGr11, 1xGr13, 4xGr16	
OGLE16aaa	TDE	9xGr13	Wyrzykowski et al. (2016)
SN2013aj	SN Ia	3xGr11, 2xGr13, 3xGr16	Maguire et al. (2013)
CSS140424-133007-212728	SN IIn	6xGr11, 1xGr13, 1xGr16	
iPTF13dge	SN Ia	4xGr11, 4xGr16	
OGLE-2014-SN-047	SN Ic	8xGr13	
LSQ14gfb	SN Ia-p	2xGr11, 4xGr13, 2xGr16	
OGLE15qz	SN Ic-p	3xGr11, 2xGr13, 3xGr16	
SN2016O	SN IIP	8xGr13	
LSQ12fhs	SN Ia-p	3xGr11, 4xGr13	
SN2012hn	SN I	3xGr11, 1xGr13, 3xGr16	Valenti et al. (2013)
SSS130404-102043-062657	SN Ia	2xGr11, 3xGr13, 2xGr16	
LSQ13sj	SN II	7xGr13	
SN2014ad	SN Ic	2xGr11, 3xGr13, 2xGr16	
OGLE-2013-SN-118	SN Ia	3xGr11, 2xGr13, 2xGr16	
LSQ13bnx	SN II	3xGr11, 1xGr13, 3xGr16	
LSQ14eez	SN I	7xGr13	
ASASSN-14kp	SN II	7xGr13	
PS15dsr	SN II	2xGr11, 3xGr13, 2xGr16	
LSQ15rw	SN IIb	7xGr13	
MASTERJ141023.42-431843.7	SN Ib	7xGr13	
Gaia16aec	SN II	7xGr13	
SN2013U	SN Ia	3xGr11, 3xGr16	Maguire et al. (2013)
LSQ14abd	SN Ia	2xGr11, 1xGr13, 3xGr16	
CSS140914-010107-101840	SN Ia	2xGr11, 2xGr13, 2xGr16	
ASASSN-15go	SN Ia	3xGr11, 3xGr16	
LSQ15abl	SN IIn-p	3xGr11, 1xGr13, 2xGr16	
OGLE15sd	SN Ic-p	5xGr11, 1xGr13	
PS15yr	SN IIb	3xGr11, 3xGr16	
AT2016bln	SN Ia-p	3xGr11, 1xGr13, 2xGr16	
OGLE-2013-SN-019	SN IIn	4xGr11, 1xGr13	
SN2012hd	SN Ia	2xGr11, 1xGr13, 2xGr16	Maguire et al. (2013)
LSQ12gxb	SN I-p	3xGr11, 1xGr13, 1xGr16	
LSQ13deg	AGN	5xGr13	
LSQ14nr	SN Ia	1xGr11, 3xGr13, 1xGr16	
CSS131031-095508+064831	SN Ia	1xGr11, 3xGr13, 1xGr16	
LSQ14eer	SN II	4xGr11, 1xGr13	

ASASSN-15hf	SN Ia	2xGr11, 1xGr13, 2xGr16	
ASASSN-15hy	SN Ia-p	2xGr11, 1xGr13, 2xGr16	
LSQ15bfp	SN Ic	5xGr13	
SN2015ay	SN II	5xGr13	
PSNJ14095513+1731556	SN Ia	1xGr11, 3xGr13, 1xGr16	
SN2016blz	SN II	2xGr11, 1xGr13, 2xGr16	
CSS121008-014245+213928	SN Ia	4xGr13	
LSQ14bdq	SN Ic	1xGr11, 3xGr13	Nicholl et al. (2015)
OGLE-2014-SN-189	unknown	3xGr11, 1xGr13	
OGLE-2014-SN-131	SN IIn-p	2xGr11, 1xGr13, 1xGr16	
CSS140925-005854+181322	SN Ic-p	4xGr13	
ASASSN-15be	SN Ia	2xGr11, 2xGr16	
OGLE-2015-SN-043	SN II	4xGr13	
CSS150124-140455+085515	SN Ia	2xGr11, 2xGr16	
ASASSN-15uo	SN IIn	2xGr11, 1xGr13, 1xGr16	
SN2016aj	SLSN-I	4xGr13	
LSQ12btw	SN Ibc	1xGr11, 1xGr13, 1xGr16	Pastorello et al. (2015b)
LSQ13der	SN Ic	3xGr13	
PSNJ11484578-2817312	SN Ic	1xGr11, 1xGr13, 1xGr16	
ASASSN-15fz	SN II	2xGr11, 1xGr16	
ASASSN-15pz	SN Ia	3xGr13	
ASASSN-15rp	SN II	3xGr13	
OGLE-2015-SN-065	SN IIn	1xGr11, 1xGr13, 1xGr16	
PS15cem	SN II	2xGr11, 1xGr13	
SN2016aqf	SN II	3xGr13	
AT2016aqs	SN Ia	3xGr13	
SN2016ado	SN Ia-p	1xGr11, 1xGr13, 1xGr16	
Gaia16afe	SN Ia-p	2xGr13, 1xGrGB	
SN2014da	SN Ia	2xGr13	
LSQ14doz	SN II-p	2xGr13	
ASASSN-15fi	SN II	2xGr13	
ASASSN-15nr	SN Ia	1xGr11, 1xGr16	
PSNJ21505094-7020289	SN Ia	1xGr11, 1xGr16	
PS15cwx	SN Ia	1xGr11, 1xGr16	
DES15S2nr	SN I-p	2xGr13	
PS15cko	SN I-p	2xGr13	
SN2013F	SN Ibc	2xGr11	
LSQ13ccw	SN Ibn	1xGr13	
PS15cel	SN II	1xGr13	Pastorello et al. (2015a)

Table 4: Total number of science files released in the various formats described here.

File type	Format	Number of files	Data Volume
EFOSC2 1D spectra	Binary Table for-mat	2851	0.13GB
EFOSC2 2D spectral images	FITS image	2851	9.18GB

SOFI 1D spectra	Binary Table for-mat	226	10.0MB
SOFI 2D spectral images	FITS image	226	0.71GB
SOFI image weights	FITS image	775	5.63GB
SOFI images	FITS image	775	5.63GB
TOTAL		7706	**21.29GB**

Data Reduction, Calibration and Quality

1. EFOSC2 Spectroscopic calibration data and reduction

Bias calibration: A set of 11 bias frames are typically taken each afternoon of PESSTO EFOSC2 observations and are used to create a nightly master bias. This nightly master bias frame is applied to all EFOSC2 data taken, including the spectroscopic frames, the acquisition images and any photometric imaging. The frame used for the bias subtraction can be tracked in the header keyword.

```
ZEROCOR = 'bias_20130402_Gr11_Free_56448.fits
```

The file name gives the date the bias frames were taken, the Grism and filter combinations for which it is applicable (of course for biases this is not relevant but the pipeline keeps track with this nomenclature) and the MJD of when the master bias was created. The dark current is less than 3.5 e– pix–1 hr–1, hence with typical PESSTO exposures being 600-1800s, no dark frame correction is made.

Flat field calibration : The PESSTO survey takes sets of spectroscopic flatfields in the afternoons at a typical frequency of once per sub-run of 3-4 nights. Five exposures are taken with maximum count levels of 40,000-50,000 ADU for each of the grism, order sorting filter, and slit width combinations that we use (8 combinations in total). Each of these is combined to give a masterflat which can be associated with the appropriate science observations from the sub-run.

```
FLATCOR = 'nflat_20130413_Gr11_Free_slit1.0_100325221_56448.fits'
```

The EFOSC2 CCD#40 is a thinned chip, hence has significant fringing beyond 7200Å and the severity depends upon the grating used. The only way to remove fringing (in spectroscopic mode) is to take a calibration flat field lamp exposure immediately after or before the science image and use this to divide into the science spectrum. PESSTO always takes internal lamp flats (3 exposures of typically 40,000 ADU maximum count level) after taking any science spectra with Gr#16. More details on the exact methods used are given in Smartt et al. (2015).

Cosmic ray removal : The PESSTO pipeline incorporates a modified version of the python implementation of LaCOSMIC (Van Dokkum 2001) to remove cosmic rays in the central 200 pixels around the object (i.e. central pixel ±100 pixels).

Arc frames and wavelength calibrations: Arc frames are taken in the evening before observing and in the morning after the night finishes. EFOSC2 has helium and argon lamps and PESSTO uses both of these lamps turned on together. No arc frames are taken during the night to reduce overheads. Although EFOSC2 suffers from

significant flexure as the instrument rotates at the nasmyth focus (which can be 4 pixels over 200 degrees in rotation), the flexure causes a rigid shift of the wavelength frame. Hence we apply the calibration determined from the evening arc frames and adjust this with a linear offset as measured from either the skylines or atmospheric absorption lines. Relatively high order Legendre polynomial fits (5-6) are needed to fit the EFOSC2 arc lines with a fit which produces no systematic residuals. The number of arc lines used for the dispersion solution of each object, along with the RMS error, are given in the header of the reduced spectra by the keywords LAMNLIN and LAMRMS respectively. The formal RMS values are probably too small to realistically represent the uncertainty in the wavelength calibration at any particular point, given the FWHM of the arclines is 13-17Å. Hence this might suggest over-fitting of the sampled points. As a comparison, Legendre polynomials with order 4 produced obvious systematic residuals and RMS values of between 0.4-1.0Å for a 1.0" slit and 1-1.8Å for a 1.''5 slit. For exposures longer than 300 s, the linear shift applied to the dispersion solution is measured from the night sky emission lines. For shorter exposures such as spectrophotometric standards, the night sky lines are not visible, and the shift is instead measured from the telluric absorptions in the extracted 1D spectrum. The linear shifts are typically in the range of 6-13 Å for Gr#11 and Gr#13. In the case of Gr#16 spectra the shifts were usually smaller, usually 4-9 Å. This value of linear shift is recorded in the header keyword SHIFT. The linear shifts are calculated by cross-correlating the observed spectrum (sky or standard) with a series of library restframe spectra which are off set by 0.1Å. The library spectrum which produces the minimum in the cross-correlation function is taken as the correct match and this shift is applied. This method limits the precision of the shift to 0.1Å, which is roughly 1/40 of a pixel and less than 1/100 of a resolution element. This value of 0.1Å is recorded in the header as the systematic error in the wavelength calibration (SPEC_SYE).

Spectrophotometric standards and flux calibration: PESSTO uses a set of 9 spectrophotometric standard stars for (see Smartt et al. 2015) and we typically observe an EFOSC2 spectrophotometric standard three times per night (start, middle and end), although if there are significant SOFI observations or weather intervenes then this may be reduced. Generally, the three observations will include 2 different stars and a set of observations is taken with all grism, slit and filter combinations used during the nights observing. To remove any second order contamination in the flux standards, PESSTO always takes Gr#13 data for these stars with and without the filter GG495, to allow correction for the effect during pipeline reductions. Flux standards are always observed unless clouds, wind or humidity force unexpected dome closure. Hence even during nights which are not photometric, flux standards are taken and the spectra are flux calibrated; we deal with the issue of the absolute flux reliability below. A sensitivity function is derived for each EFOSC2 configuration from the spectrophotometric standards observed for each night. This was then applied to the final reduced spectra. In a few instances, a sensitivity curve was not created for a particular configuration on a given night, as there were no appropriate standards observed. In these cases, the sensitivity function from the preceding or following night was used.

The standard method of ensuring spectra are properly flux calibrated is to compare synthetic photometry of the science spectra with contemporaneous calibrat-

ed photometry and apply either a constant, linear or quadratic multiplicative function to the spectra to bring the synthetic spectra into line with the photometry. For PESSTO SSDR1 this is not yet possible for all spectra since the photometric lightcurves are not yet finalised for many of the science targets and the classification spectra do not have a photometric sequence. However it is useful to know what the typical uncertainty is in any flux calibrated PESSTO spectrum, and this is encoded in the header keyword FLUXERR. PESSTO observes through non-photometric nights, and during these nights all targets are still flux calibrated. Hence the uncertainties in flux calibrations come from transparency (clouds), seeing variations that cause mismatches between sensitivity curves derived using standards with different image quality, and target slit positioning. Finally, photometric flux is generally measured with point-spread-function fitting which inherently includes an aperture correction to determine the total flux whereas spectroscopic flux is typically extracted down to 10 per cent of the peak flux (a standard practice in IRAF's apall task). All of this means that large percentage variations are expected and we carried out tests as to how well this method works and what is the reliability of the absolute flux calibration in the spectra. In Smartt et al. (2015) we describe these quantitative tests, and we have used the photometric sequence of SN2013ej to test this 2nd years data release (Yuan et al., in prep). This is illustrated in Fig. 1. We find that the RMS scatter in the absolute spectroscopic flux calibration is 36% and this is recorded in the headers of all spectra.

```
FLUXERR =                   36 /Fractional uncertainty of the flux [%]
```

Science users should use this as a typical guide, if the seeing (as can be measured on the 2D frames and acquisition images) and night conditions (from the PESSTO wiki night reports; see Smartt et al. 2015) are reasonable. In future data releases we plan to significantly improve on the flux calibration scatter by using flux calibrated acquisition images.

Telluric absorption correction: PESSTO uses a model of the atmospheric absorption to correct for the H_2O and O_2 absorption (see Smartt et al. 2015 for details). This is carried out for all grism setups. The intensities of H_2O and O_2 absorptions in the atmospheric absorption model are first Gaussian smoothed to the nominal resolution of each instrumental setup, and then rebinned to the appropriate pixel dispersion. The pipeline then scales the model spectrum so that the intensities of H_2O and O_2 absorptions match those observed in the spectrophotometric standards, hence creating multiple model telluric spectra per night. Each science spectrum is than corrected for telluric absorption, by dividing it by the smoothed, rebinned, and scaled absorption model which is most closely matched in time i.e. closest match between the standard star observation time and the science observation time.

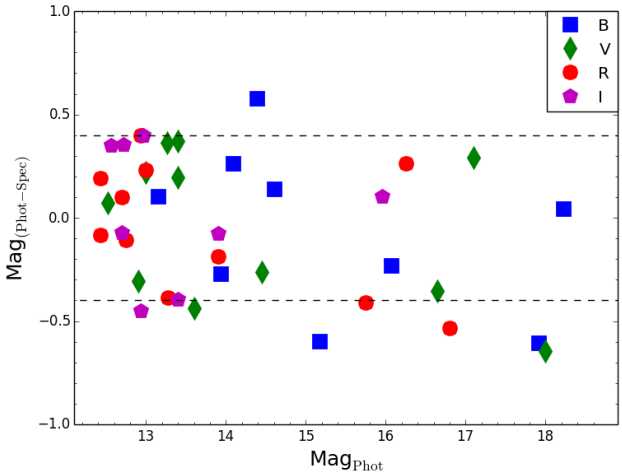

Fig 1: Synthetic magnitudes as measured from flux-calibrated spectra (Gr#11 and Gr#16) compared to the photometric magnitude at the same epoch for SN2013ej (Yuan et al., in prep.). $\mathrm{Mag_{Phot}}$ is the calibrated photometric magnitude and the y-axis is the difference between this and the synthetic photometry measured from the flux calibrated spectra. Colours and symbols indicate filters. The mean of all the values is -0.058 with a RMS of 0.360.

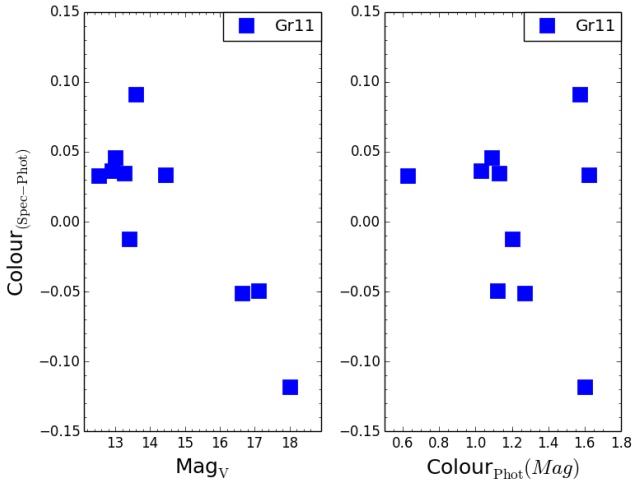

Fig 2: A check on the relative flux calibration of the PESSTO spectra. The difference between the synthetic photometry colours of SN2013ej (Gr#11) and photometric measurements is plotted on the y-axis. The x-axis is simply the V-band photometric magnitude on the left panel and photometric colour $B - V$ on the right . The colour RMS is 0.058.

2. SOFI Spectroscopic calibration data and reduction

Similar to PESSTO observations and reductions for EFOSC2, we aim to homogenise the SOFI observations and calibrations and tie them directly to what is required in the data reduction pipeline. A standard set of PESSTO OB for calibrations and science are available on the PESSTO wiki and the following sections describe how they are applied in the pipeline reduction process. An example of a fully calibrated SOFI spectrum illustrating the wavelength range and atmospheric windows is shown in Fig. 2.

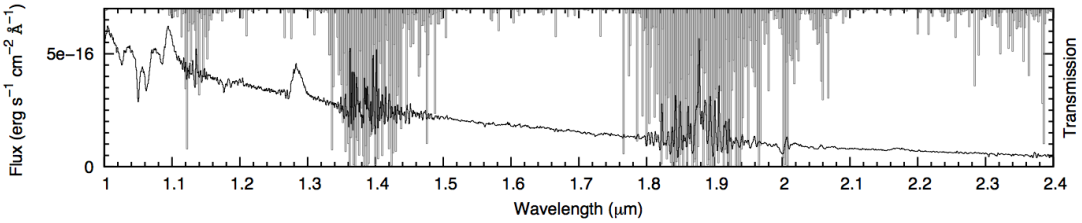

Fig 2. Combined blue and red grism SOFI spectra of SN 2012ec taken on 2013 September 24. Overplotted in grey is the atmospheric transmission, showing the correspondence between regions of low transparency and poor S/N in the spectrum.

Bias, dark and cross-talk correction: The detector bias offset and structure is subtracted along with the sky background, as is standard procedure with his chip. The SOFI detector suffers from cross talk, where a bright source on either of the two upper or lower quadrants of the detector will be accompanied by a "ghost" on the corresponding row on the opposite two quadrants. This cross-talk effect is corrected for within the PESSTO pipeline by summing each row on the detector, scaling by a constant value, and subtracting from the opposite quadrants.

Flat field calibration: The lamp-off flats are subtracted from the lamp-on flats, to remove the thermal background of the system. These subtracted flat fields are combined and normalized and used to correct for the pixel to pixel variations in detector sensitivity in the science and standard star frames. The amplitude of the variability in the flat field is ~4% for the red grism and ~6% for the blue grism. Two normalized red grism flat fields taken ~5 months apart show exactly the same structure, demonstrating that the flat field is stable, and that the use of monthly calibrations is justified (see Smartt et al. 2015).

Arc frames and wavelength calibrations : wavelength calibration is performed using spectra of a Xenon arc lamp. To fit the dispersion solution of the arc spectra without any systematic residuals requires a 4th order polynomial fit (see Table 2 for details of numbers of lines and RMS). This dispersion solution is applied to the two dimensional spectra and the sky lines are cross-correlated with an accurately calibrated template sky. A linear shift is applied to the wavelength calibration and recorded in the header keyword SHIFT. As with the EFOSC2 correction, the precision of the wavelength correction is limited to 0.1Å, due to the scale of the shifts in the library sky spectra employed. Hence this value of 0.1Å, is again recorded as the systematic error in the wavelength calibration (SPEC_SYE).

Sky subtraction and spectral extraction : SOFI spectra for PESSTO are taken in an ABBA dither pattern. This pattern consists of taking a first (A_1) exposure at a position 'A', then moving the telescope so that the target is shifted along the slit of SOFI by ~5-10 " to position 'B'. Two exposures are taken at 'B' (B_1 and B_2), before the telescope is offset back to 'A' where a final exposure (A_2) is taken. The pipeline subtracts each pair of observations (i.e, $A_1 - B_1$, B_1-A_1, B_2-A_2, A_2-B_2) to give individual bias- and sky-subtracted frames and shifts these sky-subtracted frames so that the trace of the target is at a constant pixel position, and the frames are then combined. Finally, the spectrum is optimally extracted interactively.

Telluric absorption correction : A"telluric standard" is observed immediately prior to or following the science spectrum, and at a similar airmass. The spectrum of the telluric standard is then divided by an appropriate template spectrum of the same spectral type, yielding an absorption spectrum for the telluric features. The absorption spectrum is then divided into the science spectrum to correct for the telluric absorption. As part of PESSTO, we observe either a Vega-like (spec-

tral type A0V) or a Solar analog (G2V) telluric standard for each SOFI spectrum. The PESSTO pipeline uses the closest (in time) observed telluric standard to each science or standard star spectrum.

Spectrophotometric standards and flux calibration : The process for correcting the spectrum for the telluric absorption also provides a means for flux calibration using the Hipparcos I or V photometry of the solar analogs and Vega standards used. The flux of the observed telluric standard spectrum is scaled to match the tabulated photometry, with the assumption that the telluric standards have the same color (temperature) as Vega or the Sun. A second step is performed to flux calibrate the spectra using a spectrophotometric standard. The spectrophotometric standard is reduced and corrected for telluric absorption using a telluric standard, with the same technique as used for the science targets. This corrected standard spectrum is then compared with its tabulated flux, and the science frame is then linearly scaled in flux to correct for any flux discrepancy. There are only a handful of spectrophotometric standard stars which have tabulated fluxes extending out as far as the K-band (listed in Table 2 of Smartt et al. 2015). All SOFI spectra have the following keyword which denotes which telluric standard was used for both the telluric correction and the initial flux calibration.

```
SENSFUN = 'Hip105672_20130816_GB_merge_57000_1_ex.fits' /tell stand frame
```

The spectrophotometric flux standard from Smartt et al. (2015; Table 3) used to additionally scale the flux and the keyword SENSPHOT is added to the header, with the spectrum used to apply the flux calibration. This file has the name of the standard labelled.

```
SENSPHOT= 'sens_Feige110_20130816_GB_merge_57000_1_f.fits' / sens used to flux cal
```

To improve the scaling of the absolute flux levels of the spectra, we employ the *JHKs* imaging that is normally done when SOFI spectra are taken. Synthetic *J* and *H*-band photometry was performed on the blue grism spectra, and *H* and *K*-band photometry on the red grism spectra. The magnitude offsets between the *JHK* synthetic photometry and the *JHK* aperture photometry provide scaling factors of the absolute flux levels applied to the spectra. We use the RMS of the zeropoints measured over the year as the typical uncertainty in the absolute flux calibration.

This uncertainty in the absolute flux calibration is recorded in the headers of all SOFI spectra with the following header keyword (as done for EFOSC2) :

```
FLUXERR =                22.0 /Fractional uncertainty of the flux [%]
```

3. SOFI imaging calibration frames and reduction

Bias, cross-talk and flat calibration : SOFI imaging is carried out as default when spectroscopy is done, providing images with a 4.9 arcmin field of view (0.29 arcsec pix^{-1}). The cross talk effect is first corrected as for the spectra and all images are then flat fielded using dome flats, which are typically taken on an annual basis. Pairs of flats are taken with the dome screen illuminated and un-illuminated; the latter are then subtracted from the former to account for bias and thermal background. Multiple flats are combined, and then used to reduce the science data. An illumination correction is also applied, to account for the difference between the illumination pattern of the dome flats and the actual illumination of the night sky. The illumination correction is determined by imaging a bright star at each position in a 4×4 grid on the detector. The intensity of the star is then measured at each position, and a two-dimensional polynomial is fitted. This polynomial is normalised to unity, so that it can be applied to the imaging data as a multiplicative correction

Sky subtraction : For targets that are in relatively uncrowded fields, a dither pattern is employed where the telescope is moved to four offset positions on the sky, while keeping the target in the field of view ("on-source sky subtraction"). To determine the sky background, the four frames are then median combined without applying offsets, rejecting pixels from any individual image which are more than a certain threshold above the median. This initial sky image is subtracted from each individual frame in order to obtain a initial sky-subtracted images. These frames are used to identify the positions of all sources and create a mask frame for each science image. For each set of four images, the frames are then median combined again without applying offsets and using the masks created previously to reject all sources and produce the final sky image. The final sky background image is then subtracted from each of the input frames. The sky-subtracted images are then mosaiced together to create a single image using the swarp package (Bertin et al. 2002).
For targets which are in a crowded field, or where there is extended diffuse emission (such as nearby galaxies), PESSTO observations alternate between observing the target, and observing an uncrowded off-source field around ~5 arcmin from the target (typically four frames on source, then four frames off source are observed, dithering in each case). The off-source frames are then used to compute a sky frame in the same way as for the "on-source sky subtraction". The off-source sky frame is then subtracted from each of the on-source images of the target, which are then combined to create the final image. Since the field of view of SOFI is rather small (4.9 arcmin) the astrometry is not set for single images. Instead, sextractor is run to detect sources in individual frames, and to check the nominal dither.

Astrometric calibration : The astrometric calibration was derived using the 2MASS reference catalogues, and a distortion model described by a second order polynomial. A typical scatter of 0.4-0.5 arcsec was been found for the science frames with around 15 stars usually recognised by the catalogue in the frame. This typically improves to an rms ~0.2-0.3 with ~>30 stars.. The information on the RMS of RA and DEC is provided in the standard CRDER1 and CRDER2 keywords and repeated, along with the number of stars used for the calibration, in the PESSTO-specific keyword ASTROMET.

Photometric calibration : The individual SOFI images, which themselves are the result of the average combination of NDIT images, are then mosaiced together in a median combine using swarp., An astrometric calibration is made, by cross correlating the sources detected by sextractor with the 2MASS catalogue. The instrumental aperture magnitudes of the sources in the field as measured by daophot are then compared to their catalogued 2MASS magnitudes to determine the photometric zeropoint, which is recorded in the header of the image as PHOTZP. The other relevant photometric keywords are as follows (see Smartt et al., 2015 for more details).

```
PSF_FWHM=            1.015714368/Spatial resolution (arcsec)
ELLIPTIC=                 0.142 /Average ellipticity of point sources
PHOTZP =                  25.4895217391  / MAG=-2.5*log(data)+PHOTZP
PHOTZPER=                   0.09695742781/error in PHOTZP
FLUXCAL = 'ABSOLUTE'            /Certifies the validity of PHOTZP
PHOTSYS = 'VEGA      '          / Photometric system VEGA or AB
ABMAGSAT=     11.94145459901092/Saturation limit for point sources (AB mags)
ABMAGLIM=     18.96704572844871/ 5-sigma limiting AB magnitude for point sources
```

The zeropoint conforms to ESO SDP standards for archive images and can be employed simply as :

$$MAG = -2.5\log\left(COUNTS_{ADU}\right) + PHOTZP$$

where $COUNTS_{ADU}$ is the measured signal in ADU. Users should be aware that these zeropoints are for guidance rather than for immediate and unchecked scientific use for photometry of transients. The zeropoints should always be checked with 2MASS sources, since the number and brightness of targets in automated selection various considerably due to the limited field of view of SOFI.

SOFI artifacts and problem images : The SOFI images are characterized by a number of recurring features which are mostly related to the sky subtraction method employed above. For example, Fig 3 shows an example image and its weight to illustrate the "on-source sky subtraction". Table 5 lists some specific example image issues from SOFI and the impact on their science use.

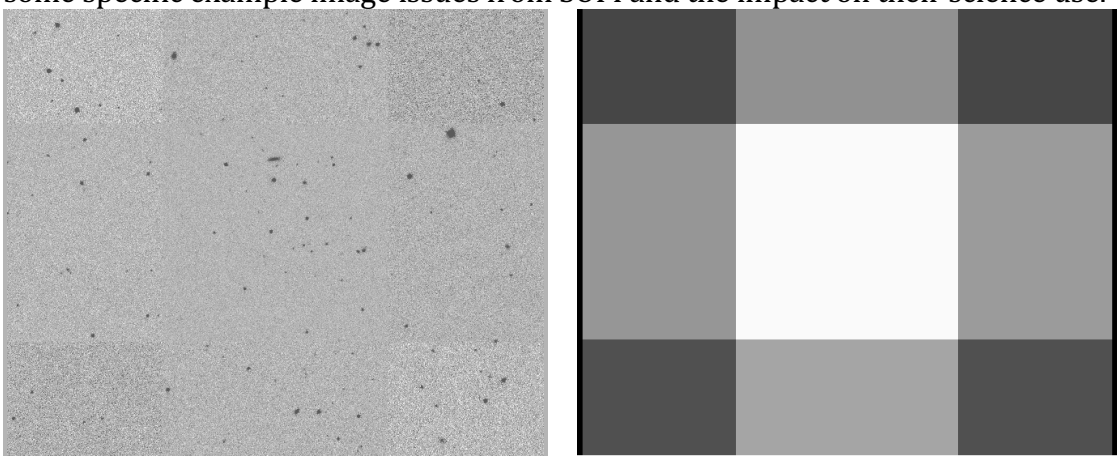

Fig 4 : the typical SOFI dither pattern for "on-source sky subtraction". The left panel shows a typical image, with the sky noise levels varying due to the dither pattern illustrated. The right panel is the weight image.

Table 5 : Specific examples of SOFI imaging issues.

Images	Description of issues
SN2009ip_20131014_Ks_merge_57050_1.fits SN2013dn_20130816_H_merge_57049_1.fits SN2013ek_20130816_H_merge_57049_1.fits SN2013fs_20131014_Ks_merge_57050_1.fits	These exemplify cases where there are vertical noise patterns in the background, likely electronic in origin. However the middle region around the transient is typically less affected. These four are examples, there are others with similar background patterns.
OGLE-2013-SN-079_20131025_J_merge_57050_1.fits SN2013ek_20130828_J_merge_57049_1.fits SN2013fc_20131013_H_merge_57050_1.fits SN2013fc_20131209_Ks_merge_57050_1.fits	These exemplify cases where there are residuals from the bright host galaxy, when the offsets were used. This reflects

	the higher noise levels where the galaxy was shifted in the dither pattern. However the region around the transient should be unaffected. These four are examples, there are others with similar background patterns.
SN2012ca_20131102_H_merge_57050_1.fits SN2012ca_20131102_J_merge_57050_1.fits SN2013fc_20131003_H_merge_57050_2.fits SN2013fc_20131209_H_merge_57050_1.fits	Poor image, reason not known. Use with caution
SN2013ek_20130816_Ks_merge_57049_1.fits LSQ13ddu_20131209_H_merge_57050_1.fits	Core of a bright galaxy/star saturated. When the dithered offsets were used for sky subtraction, this prints through. However, the SN position should be unaffected. These two are examples, there are others with similar background patterns.

Previous Releases

Release number 2 contained flux-calibrated 1d EFOSC spectra of all targets taken during the first year (between April 2012 and April 2013), plus SOFI 1d spectra and imaging products for the brightest targets.

Release number 3 contains all the products of release number 2 plus the 1d spectra and images of the targets taken during the second year (between August 2013 and April 2014).

List of Spectral Changes

.

1. Spectrum for object SN2103ek was re-uploaded to correct its object name to 'SN2013ek'.
2. Spectrum for object MASTER134201m023856 was re-uploaded to correct its object name to 'MASTERJ134201.21-023856.2'
3. Spectrum for object MASTEROTJ093953.18+165516.4 was re-uploaded to correct its object name to 'MASTERJ093953.18+165516.4'
4. Spectrum for object OGLE-2012_SN-027 was re-uploaded to correct its object name to 'OGLE-2012-SN-027'

5. Spectrum for object OGLE2013-SN-017 was re-uploaded to correct its object name to 'OGLE-2013-SN-017'
6. Spectrum for object PSNJ125333062742517 was re-uploaded to correct its object name to 'PSNJ12533306+2742517'
7. Spectrum for object PSNJ02554120-2725276 was re-uploaded to update its object name to 'SN2012fx'
8. Spectrum for object PSNJ04371913-6908254 was re-uploaded to update its object name to 'SN2012fu'
9. Spectrum for object PSNJ081753462328105 was re-uploaded to update its object name to 'SN2013gq'
10. Spectrum for object PSNJ09040080-7203248 was re-uploaded to update its object name to 'SN2013B'
11. Spectrum for object PSNJ19065165-6142163 was re-uploaded to update its object name to 'SN2012fv'
12. Spectrum for object PSNJ20032484-5557192 was re-uploaded to update its object name to 'SN2012fz'
13. Spectrum for object PSNJ21015899-4816259 was re-uploaded to update its object name to 'SN2012fw'
14. Spectrum for object PSNJ23054871+1419564 was re-uploaded to update its object name to 'SN2012ff'
15. Spectrum for object sn2012fs was re-uploaded to correct its object name to 'SN2012fs'
16. Spectrum for object SSS121120-023241-391756 was re-uploaded to update its object name to 'SN2012hc'

Release number 4 contains all the products of release number 3 plus the 1d spectra and images of the targets taken during the third and forth years (between July 2014 and April 2016).

List of Spectral Changes

1. Spectrum for object SN2013gr taken on 21031221 was re-uploaded as the extracted source was that of the host galaxy and not the supernova.

Data Format

1. EFOSC2 data file types and naming

One dimensional flux calibrated spectra are in binary table format and conform to the ESO Science Data Products Standard (Retzlaff et al. 2013). The binary table FITS file consists of one primary header (there is no data in the primary HDU so NAXIS=0), and a single extension containing a header unit and a BINTABLE with NAXIS=2. A unique FITS file is provided for each individual science spectrum. The actual spectral data is stored within the table as vector arrays in single cells. As a consequence, there is only one row in the BINTABLE, that is NAXIS2=1.
Information associated with the science spectrum is also provided within the same binary table FITS file resulting in a table containing one row with four data cells. The first cell contains the wavelength array in angstroms. The other three cells contain the science spectrum flux array (extracted with variance weighting), its error array (the standard deviation produced during the extraction procedure) and finally the sky background flux array. Each flux array is in units of erg cm^{-2} s^{-1} $Å^{-1}$.

The science spectrum has a filename of the following form, object name, date of observation, grism, filter, slit width, MJD of data reduction date, a numeric counter (beginning at 1) to distinguish multiple exposures taken on the same night, and a suffix `sb` to denote a spectrum in binary table format.

```
SN2013ak_20130412_Gr11_Free_slit1.0_56448_1_sb.fits
```

In the few cases where the object name is longer than 20 characters, it is truncated within the filename to ensure the filename does not exceed the 68 character limit enforced by ESO. The full object name is always recorded in the OBJECT keyword.

They can be identified as having the data product category keyword set as

```
PRODCATG = SCIENCE.SPECTRUM /Data product category
```

The 2D spectrum images which can be used to re-extract the object as discussed above are released as associated ancillary data. They are associated with the science spectra through the following header keywords in the science spectra files. The file name is the same as for the 1D spectrum, but the suffix used is `i` to denote an image.

```
ASSOC1 = ANCILLARY.2DSPECTRUM          /Category of associated file
ASSON1 = SN2013ak_20130412_Gr11_Free_slit1.0_56448_1_si.fits /Name of associated file
```

These 2D files are wavelength and flux calibrated hence a user can re-extract a region of the data and have a calibrated spectrum immediately. Users should note the value for `BUNIT` in these frames means that the flux should be divided by 10^{20} to provide the result in erg cm^{-2} s^{-1} Å^{-1}.

2. SOFI data file types and naming

The data products for SOFI are similar to those described above for EFOSC2. The spectra are in binary table FITS format, with the same four data cells corresponding to the wavelength in angstroms, the weighted science spectrum and its error and the sky background flux array. Again, each flux array is in units of erg cm^{-2} s^{-1} Å^{-1}. The SSDR1 FITS keywords described Smartt et al. (2015) are again applicable here. A typical file name is

```
SN2009ip_20130417_GB_merge_56478_1_sb.fits
```

Where the object name is followed by the date observed, the grism (GB for the blue grism, or GR for the red grism), the word "merge" to note that that the individual exposures in the ABBA dither pattern have been co-added, the date the file was created, a numeric value to distinguish multiple exposures on the same night and a suffix `sb` to denote a spectrum in binary table format. As with EFOSC2, this science spectrum can be identified with the label:

```
PRODCATG = SCIENCE.SPECTRUM /Data product category
```

We also provide the 2D flux calibrated and wavelength calibrated file so that users can re-extract their object directly, as described with EFOSC2. The identification of the 2D images follow the same convention as for EFOSC2, with the suffix `si` to denote a spectral image.

```
ASSOC1 = ANCILLARY.2DSPECTRUM          /Category of associated file
ASSON1 = SN2009ip_20130417_GB_merge_56478_1_si.fits /Name of associated file
```

In nearly all cases where PESSTO takes a SOFI spectrum, imaging in JHK$_S$ is also taken. These images are flux and astrometrically calibrated and released as science frames. They are labeled as follows where K$_S$ labels the filter and the `merge` denotes that the dithers have been median combined.

```
SN2013am_20130417_Ks_merge_56475_1.fits
```

We also release the image weight map as described in (Retzlaff et al. 2013). The definition in this document is the pixel-to-pixel variation of the statistical significance of the image array in terms of a number that is proportional to the inverse variance of the background, i.e. not including the Poisson noise of sources. This is labelled as

```
ASSOC1 = ANCILLARY.WEIGHTMAP          /Category of associated file
ASSON1 = SN2013am_20130417_Ks_merge_56475_1.weight.fits /Name of associated file
```

Acknowledgements

If using these data, please cite this paper

Smartt S.J. et al. 2015, A&A, 579, 40: PESSTO: survey description and products from the first data release of the Public ESO Spectroscopic Survey of Transient Objects

And please also add the following acknowledging statement in your articles

Based on data products from observations made with ESO Telescopes at the La Silla Paranal Observatory under programmes 188.D-3003 and 191.D-0935: PESSTO (the Public ESO Spectroscopic Survey for Transient Objects).

References

Barabarino C. et al., 2015, MNRAS, 448, 2312
Bennetti S., et al., 2014, MNRAS, 441, 289
Bertin, E., Mellier, Y., Radovich, M., et al. 2002, in Astronomical Society of the Pacific Conference Series, Vol. 281, Astronomical Data Analysis Software and Systems XI, ed. D. A. Bohlender, D. Durand, & T. H. Handley, 228
Childress M., et al. 2013, ApJ, 770, 29
Childress M., et al. 2015, MNRAS, 454, 3816
Fraser M., et al. 2013, MNRAS, 433, 1312
Fraser M., et al. 2015, MNRAS, 453, 3886
Gall E. E. E., et al. 2015, A&A, 582, A3
Hosseinzadeh G., et al. 2016, ApJ, in press, arXiv:1608.01998
Inserra, C., et al. 2013, MNRAS, 770, 128
Inserra, C., et al. 2013, MNRAS, 459, 2721
Inserra C., et al. 2016, ApJ, submitted, arXiv:1604.01226
Jerkstrand A., et al., 2015, MNRAS, 448, 2482
Jerkstrand A., et al., 2016, ApJ, arXiv:1608.02994
Jester et al. 2005, AJ, 130, 873
Kangas T., et al. 2016, MNRAS, 456, 323
Magee M., et al., 2016, A&A, 589, A89
Maguire K., et al. 2013, MNRAS, 436, 222
Maund J.R. et al. 2013, MNRAS, 431, L102

Nicholl et al. 2014, MNRAS, 444, 2096
Nicholl M., et al. 2015, ApJ, 807, L18
Nicholl M., et al. 2016a, ApJ, 826, 39
Nicholl M., et al. 2016b, ApJ, in press, arXiv:1608.02995
Pastorello A., et al. 2015a, MNRAS, 449, 1941
Pastorello A., et al. 2015b, MNRAS, 449, 1954
Polshaw J., et al. 2016, A&A, 58, A177
Retzlaff et al. 2013, GEN-SPE-ESO-33000-5335, Issue 5
Scalzo R., et al. 2014, MNRAS, 445, 30
Smartt S.J. et al. 2015, A&A, 579, 40
van Dokkum, P. G. 2001, PASP, 113, 1420
Yaun F. et al. 2016, MNRAS, 461, 2003
Wyrzykowski L., et al., MNRAS, submitted